

Impact of different driving cycles and operating conditions on CO2 emissions and energy management strategies of a Euro-6 hybrid electric vehicle

Original

Impact of different driving cycles and operating conditions on CO2 emissions and energy management strategies of a Euro-6 hybrid electric vehicle / Cubito, Claudio; Millo, Federico; Boccardo, Giulio; DI PIERRO, Giuseppe; Biagio, Ciuffo; Georgios, Fontaras; Simone, Serra; Marcos Otura Garcia And Germana, Trentadue. - In: ENERGIES. - ISSN 1996-1073. - STAMPA. - 10:(2017). [10.3390/en10101590]

Availability:

This version is available at: 11583/2688763 since: 2017-10-31T18:17:24Z

Publisher:

MDPI

Published

DOI:10.3390/en10101590

Terms of use:




This article is made available under terms and conditions as specified in the corresponding bibliographic description in the repository

Publisher copyright

(Article begins on next page)

Article

Impact of Different Driving Cycles and Operating Conditions on CO₂ Emissions and Energy Management Strategies of a Euro-6 Hybrid Electric Vehicle

Claudio Cubito ¹ , Federico Millo ^{1,*}, Giulio Boccardo ¹, Giuseppe Di Piero ¹ , Biagio Ciuffo ², Georgios Fontaras ², Simone Serra ² , Marcos Otura Garcia ² and Germana Trentadue ²

¹ Department of Energy, Politecnico di Torino, Corso Duca degli Abruzzi 24, 10129 Torino, Italy; claudio.cubito@polito.it (C.C.); giulio.boccardo@polito.it (G.B.); giuseppe.dipierro@polito.it (G.D.P.)

² Joint Research Centre—European Commission, Via Enrico Fermi 2749, 21027 Ispra, Italy; Biagio.CIUFFO@ec.europa.eu (B.C.); Georgios.FONTARAS@ec.europa.eu (G.F.); Simone.SERRA@ec.europa.eu (S.S.); marcos.otura@ec.europa.eu (M.O.G.); germana.trentadue@ec.europa.eu (G.T.)

* Correspondence: federico.millo@polito.it; Tel.: +39-011-090-4517

Received: 29 August 2017; Accepted: 26 September 2017; Published: 13 October 2017

Abstract: Although Hybrid Electric Vehicles (HEVs) represent one of the key technologies to reduce CO₂ emissions, their effective potential in real world driving conditions strongly depends on the performance of their Energy Management System (EMS) and on its capability to maximize the efficiency of the powertrain in real life as well as during Type Approval (TA) tests. Attempting to close the gap between TA and real world CO₂ emissions, the European Commission has decided to introduce from September 2017 the Worldwide Harmonized Light duty Test Procedure (WLTP), replacing the previous procedure based on the New European Driving Cycle (NEDC). The aim of this work is the analysis of the impact of different driving cycles and operating conditions on CO₂ emissions and on energy management strategies of a Euro-6 HEV through the limited number of information available from the chassis dyno tests. The vehicle was tested considering different initial battery State of Charge (SOC), ranging from 40% to 65%, and engine coolant temperatures, from −7 °C to 70 °C. The change of test conditions from NEDC to WLTP was shown to lead to a significant reduction of the electric drive and to about a 30% increase of CO₂ emissions. However, since the specific energy demand of WLTP is about 50% higher than that of NEDC, these results demonstrate that the EMS strategies of the tested vehicle can achieve, in test conditions closer to real life, even higher efficiency levels than those that are currently evaluated on the NEDC, and prove the effectiveness of HEV technology to reduce CO₂ emissions.

Keywords: Hybrid Electric Vehicles; CO₂ emissions; WLTP; NEDC

1. Introduction

Increasing environmental awareness has been a key driver during the past two decades for the introduction of stricter regulations for the control of pollutant and CO₂ emissions from passenger cars. In particular the European Union (EU) has committed to reducing greenhouse gas emissions from road transport by 60% by 2050 compared to 1990 levels [1]. To meet these challenging CO₂ targets, vehicle manufacturers, while relentlessly continuing the research for more efficient powertrains based on Internal Combustion Engines (ICEs), have been developing new technologies such as Electric Vehicles (EVs) and Fuel Cells Vehicles (FCEVs), which can both provide the benefits of zero tail pipe emissions

and can rely on the production of electricity and hydrogen from renewable energy sources [2–6]. However, the market penetration of these new technologies is still quite limited, struggling with often inadequate range capabilities, high costs and lack of infrastructures [7–11].

In this framework Hybrid Electric Vehicles (HEVs) represent an extremely promising solution for the automotive industry to bridge the gap between the desirable features of electric powertrains, the range capability and the more affordable costs of conventional vehicles, because they can ensure higher fuel efficiency and lower pollutant emissions compared to conventional powertrains due to the flexibility provided by the integration of the ICE with the electric powertrain, while still maintaining comparable range capabilities and costs [12,13]. However, the effective potential of HEVs in terms of CO₂ emissions reduction in real world driving conditions strongly depends on the performance of their Energy Management System (EMS) [14–16] and on its capability to maximize the efficiency of the powertrain in real life as well as in the chassis dyno tests, which are prescribed for Type Approval (TA).

Moreover, since the procedure used to date in Europe for TA [17,18], based on the New European Driving Cycle (NEDC), has been widely criticized and it has been proved to be not representative of real world driving conditions [19,20], the European Commission has decided to introduce from September 2017 the Worldwide Harmonized Light duty Test Procedure (WLTP) [21], replacing the previous procedure in an attempt to close the gap between TA and real world CO₂ emissions. The introduction of the WLTP will bring several testing and procedural changes compared to the NEDC, but how this will affect the evaluation of the CO₂ reduction potential of HEVs has not yet been fully explored. Very limited number of studies provide experimental evidence of the impact of the introduction of the WLTP on CO₂ emissions from HEVs [22–24].

Within this context, the aim of this work is the analysis of the impact of different driving cycles and operating conditions on CO₂ emissions and EMS strategies of a Euro-6 HEV. The vehicle measurements were carried out over both the NEDC and the Worldwide Harmonized Light duty Test Cycle (WLTC), which is the reference cycle of the WLTP procedure described in [21]. The characterization of the vehicle EMS was carried out through the limited amount of information available from the TA test, without any detailed characterization of the high voltage battery, the electric machines and the ICE [22,24–26].

After presenting the testing methods and procedures in Section 2 (Methodology), the effects of the new test procedure on CO₂ emissions and on the performance of the EMS at different SOC levels, ranging from 40 to 65%, and engine thermal states, from -7 °C to 70 °C, are reported in Section 3 (Results). Finally, the main findings of the work are summarized in Section 4 (Conclusions), highlighting how the change of test conditions from NEDC to WLTP led to an important increase of the specific energy demand of about 50%, and to a corresponding increase of CO₂ emissions of about 30%, thus demonstrating that the EMS strategies of the tested vehicle can achieve, in test conditions closer to real life, even higher efficiency levels than those which are currently evaluated on the NEDC.

2. Methodology

2.1. Tested Vehicle

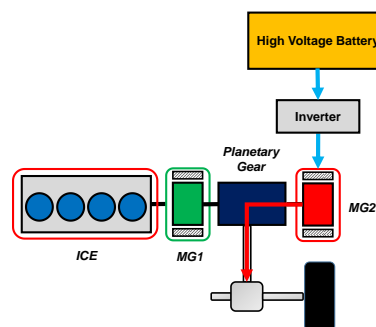
The B-Segment HEV features a complex hybrid powertrain, in which an Electric Continuous Variable Transmission (eCVT) is coupled with a Spark Ignition (SI) engine. The main vehicle characteristics are listed in Table 1. In the eCVT system the rotational shaft of the planetary gear carrier is directly linked to engine and it transmits the motive power to the outer ring gear and the inner sun gear via pinion gears. The ICE is a four-cylinder in-line 1.5 L naturally aspirated gasoline with a maximum power of 55 kW at 4800 rpm. The rotational shaft of the ring gear is directly linked to the 45 kW Motor Generator 2 (MG2) and it transmits the drive force to the wheels, while the rotational shaft of the sun gear is directly linked to the electric generator (MG1) [27]. The high voltage battery is a nickel metal hydride unit (NiMH) containing 120 cells connected in series.

Table 1. Vehicle and powertrain main characteristics [27].

Technical Data	
Curb Mass	1120 kg
Gross Mass	1565 kg
ICE	Spark Ignition Naturally Aspirated Displacement: 1.5 L Rated power: 55 kW @ 4800 rpm Rated torque: 111 Nm @ 3600–4800 rpm
MG1-MG2	Permanent Magnet Synchronous motor Maximum output power: 45 kW Maximum output torque: 169 Nm
Battery	Type: NiMH Capacity: 6.5 Ah Nominal voltage: 144 V Energy: 1 kWh

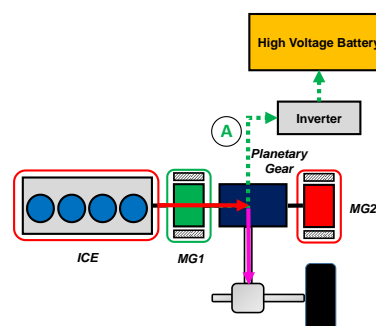
The vehicle can operate in two different modes, depending on the vehicle speed, power demand and battery SOC [27]:

1. *Electric Vehicle (EV)*: whenever the ICE would operate in an inefficient range, such as at very low load levels, the ICE is turned off and the traction power is demanded to the MG2, as illustrated in Figure 1;

**Figure 1.** EV mode.

2. *Parallel Hybrid (PH)*: at higher load levels the ICE is enabled and it supports the vehicle driving, allowing the powertrain to operate in two different ways depending on battery SOC and on the accelerator pedal position:

- *Smart Charge (SC)*: the ICE operating points are shifted at higher load levels than those required for the vehicle propulsion, closer to the optimal efficiency area, and the power exceeding the vehicle propulsion needs is used to recharge the battery through the generator MG1, as depicted in Figure 2 by the path “A”;

**Figure 2.** SC mode.

- *Electric Boost (E-Boost)*: in order to support the engine during sudden load demands, the high voltage battery provides an extra power contribution to the MG2, represented by the path “B”, as illustrated in Figure 3.

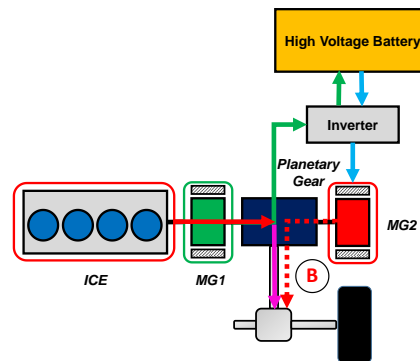


Figure 3. E-Boost mode.

2.2. Test Conditions

The experimental testing campaign was carried out at the Vehicle Emission Laboratory (VELA) of the Joint Research Centre (JRC). The test rig is equipped with a four wheel-drive (4WD) chassis dynamometer, made of two roller benches with a diameter of 48 inches (1.219 m). The chassis dyno, located in a climatic chamber, allows a maximum traction torque of 3300 Nm and the vehicle mass range permitted varies from 454 to 2720 kg. During the tests CO₂ and pollutants emissions, as well as measurements on the engine and on the battery were recorded. Engine operating parameters, such as the revolution speed and the coolant temperature, were acquired using an On Board Diagnostic (OBD) scan tool. Instead, the battery current and voltage were acquired using a Yokogawa WT1800 precision power analyzer, thanks to the direct access to the battery terminals [27].

The WLTC and NEDC driving cycles were used for the chassis testing [17,21]. As far as the WLTC is concerned, the Class-3 was adopted, since the vehicle characteristics correspond to the highest power to mass ratio. Road Loads (RLs) and test mass definitions prescribed in [17,21] were applied to the NEDC tests. As for the WLTC tests, requirements of RLs and test mass follow the WLTP regulation [21]. Coast down coefficients adopted for the two driving cycles are listed in Table 2.

Table 2. Vehicle test conditions [27].

		Unit	NEDC	WLTP
Test Mass	-	kg	1130	1325
Coast	F0	N	61	120.5
Down	F1	N/(km/h)	0.19	0.33
Coefficients	F2	N/(km/h) ²	0.0269	0.0302

An important difference between the WLTP and NEDC procedures is the substantial increase of the energy demand, as shown in Figure 4, which illustrates both the traction specific energy (i.e., the integral of the positive traction power requested along the entire cycle referred to the travelled distance) and the brake specific energy (i.e., the integral of the negative power requested during the entire cycle referred to the travelled distance).

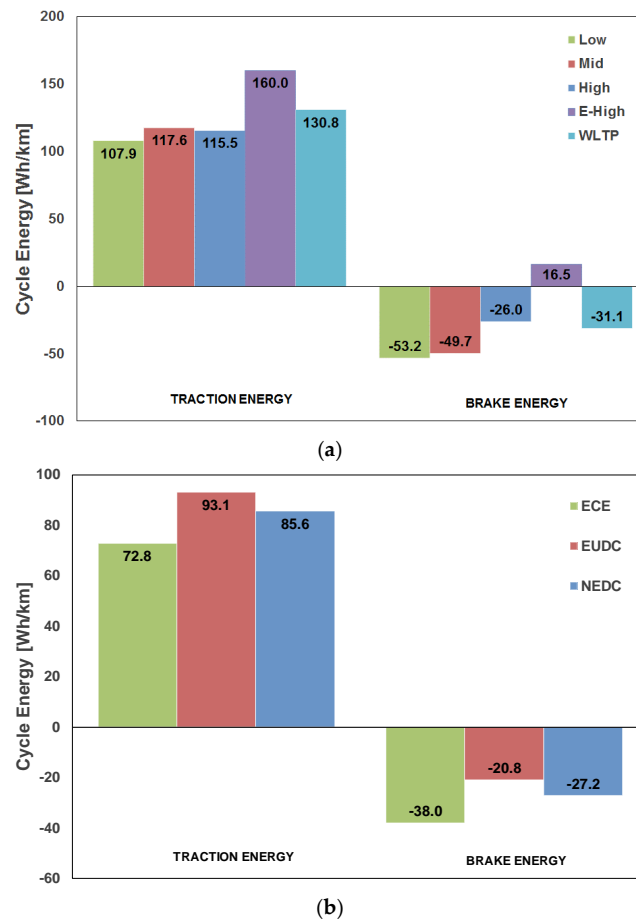


Figure 4. Traction energy demand and brake energy demand along the WLTC (a) and NEDC (b): for each driving cycle the values of the different phases (Low, Medium, High and Extra-High for WLTC and ECE and EUDC for NEDC) and for the whole cycle are shown.

An increase of about 50% in the traction specific energy demand when moving from the NEDC to the WLTP can be clearly noticed, while the brake energy only increases by than 15%, showing reduced opportunities for the exploitation of regenerative braking.

2.3. Test Protocol

The vehicle was tested under different initial battery State of Charge (SOC) conditions over both driving cycles. This aspect is of crucial importance for a HEV, because the battery works as an energy buffer, since the electric energy, which is used during the discharge phase, has then to be supplied backwards through the SC or through regenerative braking. Therefore, the same cycle was tested considering two opposite initial SOC conditions: battery fully charged (or “High SOC”) and fully discharged (“Low SOC”). It is worth to point out that the terms “High SOC” and “Low SOC” are referred to the usual range of exploitation of NiMH batteries, which ranges from a maximum of 70% to a minimum of 30% [28–30]. The battery conditioning was performed by driving at constant speed on the chassis dynamometer until the complete charge or discharge of the battery was achieved. The evolution of the battery energy level was monitored through the battery indicator on the cockpit [27].

Moreover, the vehicle was tested considering different thermal states of the ICE to appreciate the effect of coolant temperature on the EMS logic, combined with different SOC levels at the beginning of the cycle, as summarized in Table 3. Along the NEDC and WLTC cycles, the vehicle tests were carried out considering the initial coolant temperature at 25 °C, referred as “Cold”, and at 70 °C, referred as

“Hot”. Finally, to further extend the characterization of the EMS logic, a coolant temperature of -7°C was considered for the WLTC only.

Table 3. Test matrix.

SOC	NEDC		WLTC	
	High	Low	High	Low
-7°C	-	-	x	x
COLD	x	x	x	x
HOT	x	x	x	x

3. Results

The first part of this section focuses on the impact of WLTP procedure on CO_2 emissions for different battery SOC levels and engine thermal states, providing a preliminary analysis of the EMS behavior under different operating conditions. Thereafter, the EMS logic was investigated with a higher detail level, detecting the engine enabling logic and the actuation of the SC/E-boost, depending on the battery SOC, vehicle speed and acceleration. Then, the effects of the Cold start event on the control logic were investigated through the comparison with vehicle tests performed with the engine coolant temperature around 70°C .

3.1. CO_2 Emissions

The WLTP procedure, as already shown in previous Section 2.2, is more energy demanding compared to the current NEDC based TA procedure. Therefore, it is expected to lead to an increase of the overall CO_2 emissions, as already reported in literature for vehicles equipped with conventional powertrains [31,32] This section provides an additional contribution, analyzing the impact of the new TA procedure on a test case vehicle representative of current state of the art of the hybrid technology.

The CO_2 emissions measured after a Cold start, as required by the TA procedures, are shown in Figure 5 for the two different SOC levels: the WLTP procedure leads to an average increase of CO_2 emissions of 26 g/km corresponding to about a 30% increase, almost independently from the starting SOC level. Instead, the different initial battery level causes a variation of about 6 g/km of CO_2 emissions for the same driving cycle [27].

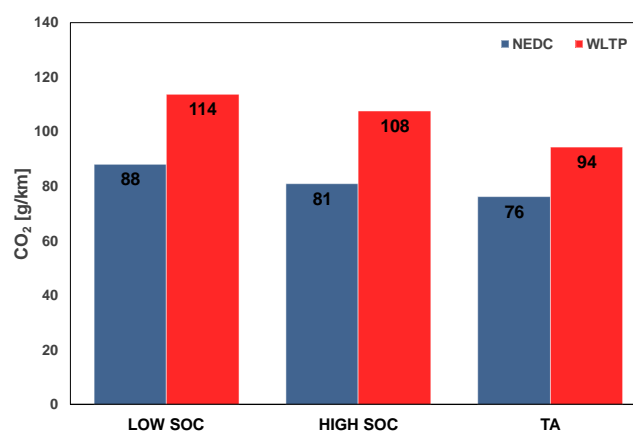


Figure 5. Cold start— CO_2 emissions according to the WLTP and NEDC procedures for the Low SOC, High SOC and TA cases.

However, as it will be shown in more details in the following section, both under Low SOC and High SOC conditions, the EMS promotes a quite aggressive battery recharging for both driving cycles, leading to SOC values at the end of the driving cycles significantly higher than the values recorded at cycle start. Therefore, the computation of the CO_2 emissions should take into account that a fraction of

the fuel energy consumed was used to increase the energy content of the battery, and not for vehicle traction. A correction factor, named “K factor”, should be applied to the measured CO₂ emissions, as prescribed by the regulations [18,21], in order to obtain the TA CO₂ values shown in Figure 5. These two values correspond to the CO₂ emissions that would be measured in case of a neutral battery energy balance (in other words with SOC level at cycle end equal to SOC level at cycle start). As far as TA CO₂ emissions are concerned, passing from NEDC to WLTP an increase of 18 g/km, corresponding to about 23%, was observed, which is noticeably lower than the increases measured for both the Low SOC and High SOC conditions.

The effects of the ICE thermal status at the start of the driving cycle are reported in Figure 6, considering only the High SOC as reference case. As already pointed out in literature [33] for conventional powertrains, the effect of Cold start on CO₂ emissions is reduced passing from NEDC to WLTP also for the hybrid powertrain. The CO₂ penalty is limited thanks to the higher power demand of the WLTP, permitting a more rapid ICE warm up compared with the NEDC, and thanks to the longer duration of the WLTC driving cycle, since the relative weight of the higher fuel consumption during the warm-up phase is significantly reduced. As a result, CO₂ emissions increase by only 4 g/km, corresponding to a percentage growth slightly lower than 4%, when passing from Cold to Hot start conditions for the WLTP, while for the NEDC an increase of about 10 g/km, corresponding to about 12%, from Cold to Hot was registered.

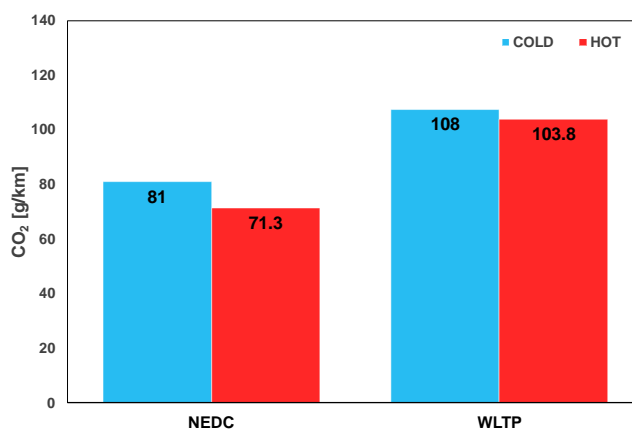


Figure 6. Effect of the Cold start on CO₂ emissions along the NEDC and WLTP cycles for the High SOC case.

Finally, the effect of extremely low temperatures on CO₂ emissions along the WLTC cycle was investigated for different SOC levels, as reported in Figure 7.

The emissions increase passing from Cold case to -7 °C case is of about 16.5% for the Low SOC case, and of about 21% for the High SOC case. It is worth pointing out that the initial battery SOC level has a very limited effect on CO₂ emissions at -7 °C, since the increase from the High to the Low SOC case is lower than 2 g/km, which is significantly less than the 6 g/km increment measured for the Cold start case (see again results shown in Figure 5). This result suggests a limited influence of the initial SOC level on the exploitation of the electric drive at -7 °C, which could be explained by the need to keep the ICE switched on to obtain a fast warm-up, regardless of the need to charge the battery.

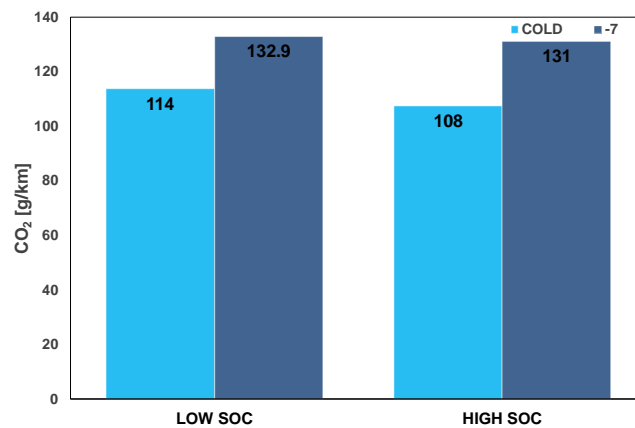


Figure 7. Impact on CO₂ emissions of -7°C test for the Low SOC and High SOC cases along the WLTC.

3.2. Analysis of the EMS Logic

This section presents a detailed analysis of the EMS logics for the two different SOC levels, using the limited amount of information available from the chassis dyno tests. The investigation procedure correlated the vehicle operating conditions such as the vehicle speed, acceleration and motive power to identify the engine enabling strategy and the use of peculiar operating modes of hybrid powertrains, such as the SC and the E-Boost [27]. Figures 8 and 9 illustrate the ICE On/Off logic, represented as Boolean variable (0 = Off, 1 = On), on a time basis, along with the battery SOC for the two different initial levels along the WLTC and NEDC cycles.

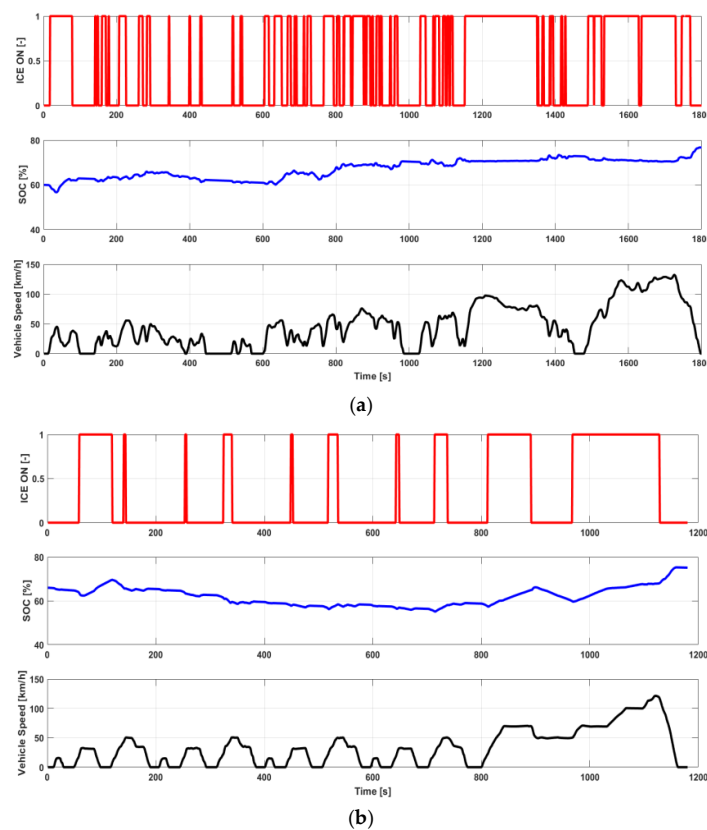


Figure 8. High SOC Cold start: ICE On/Off status, battery SOC and vehicle speed over the WLTC (a) and the NEDC (b).

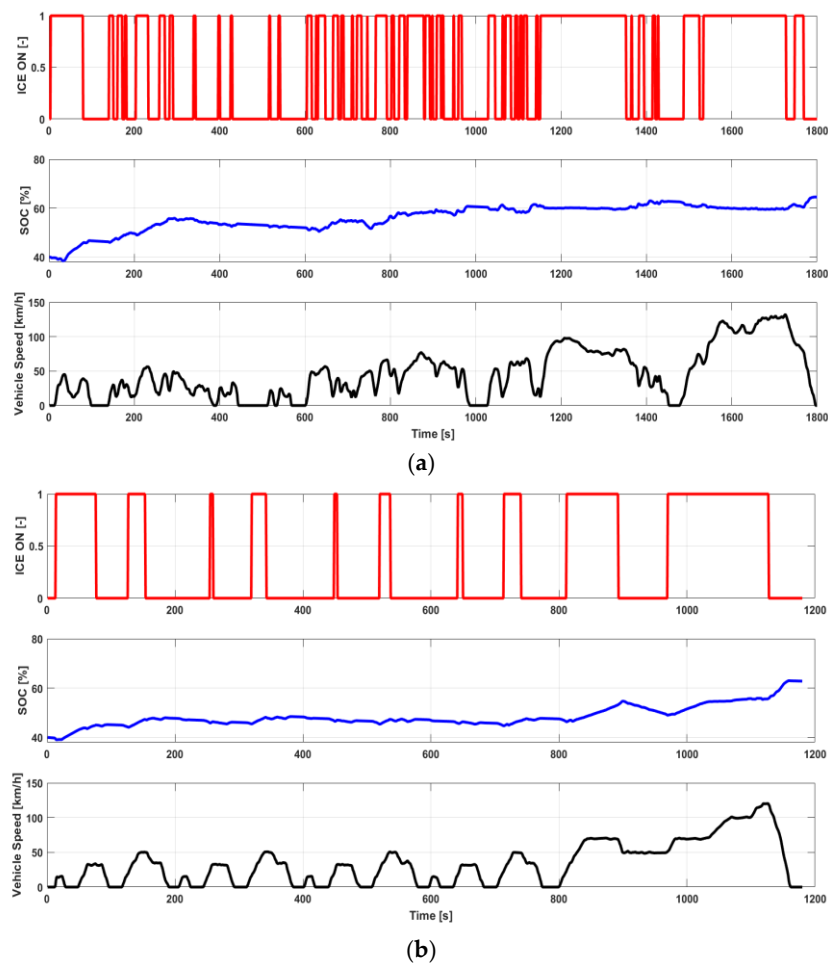


Figure 9. Low SOC Cold start: ICE On/Off status, battery SOC and vehicle speed over the WLTC (a) and the NEDC (b).

From Figure 8, which refers to the High SOC case, it is evident that the EMS permits all-electric driving only at low/medium vehicle speeds and for low accelerations, which happens when the power demand is quite limited. Therefore, the usage of the ICE is more frequent over the WLTC than over the NEDC, due to the higher power demand. Moreover, in the High SOC case it can be observed that the battery charge increases by about 15% on WLTC and by about 10% on NEDC, highlighting the frequent exploitation of the SC to increase the load of the ICE and consequently its efficiency, well beyond the need to keep the battery energy at a constant level.

In the Low SOC case, depicted in Figure 9, the ICE is more frequently enabled in the first portion of the driving cycles (particularly on the NEDC), enabling a fast battery recharge until the reaching of “normal” operating conditions (about 55% of SOC), after which the EMS tends to operate in a similar way to the High SOC case.

Moreover, even though the power demand is quite low during the initial phases of both cycles, Figures 8 and 9 show that the engine is On for approximately 100 s, probably to warm-up the after-treatment system.

However, for better understanding the EMS logic a deeper investigation of the correlation between the driving conditions and the hybrid powertrain operating modes is necessary. Therefore, the battery and the engine measurements were correlated with vehicle kinematic and dynamic measurements, such as vehicle speed, vehicle acceleration and traction power [27].

Figure 10 reports the ICE status (On/Off) for all the operating points recorded over the WLTC as a function of battery SOC and traction power. The cross and diamond markers represent respectively

the ICE Off and On conditions, while the “Start” arrow identifies the battery initial SOC on the x -axis. It can be clearly seen that in both cases the EMS enables the electric driving (corresponding to the “ICE Off” conditions) up to 10 kW. Moreover, for both cases the ICE cut-off during vehicle deceleration and the stop-start functionalities are both disabled at the beginning of the cycle to accelerate the engine and after-treatment system warm-up, as it can be inferred from the presence of ICE On points in the negative power region.

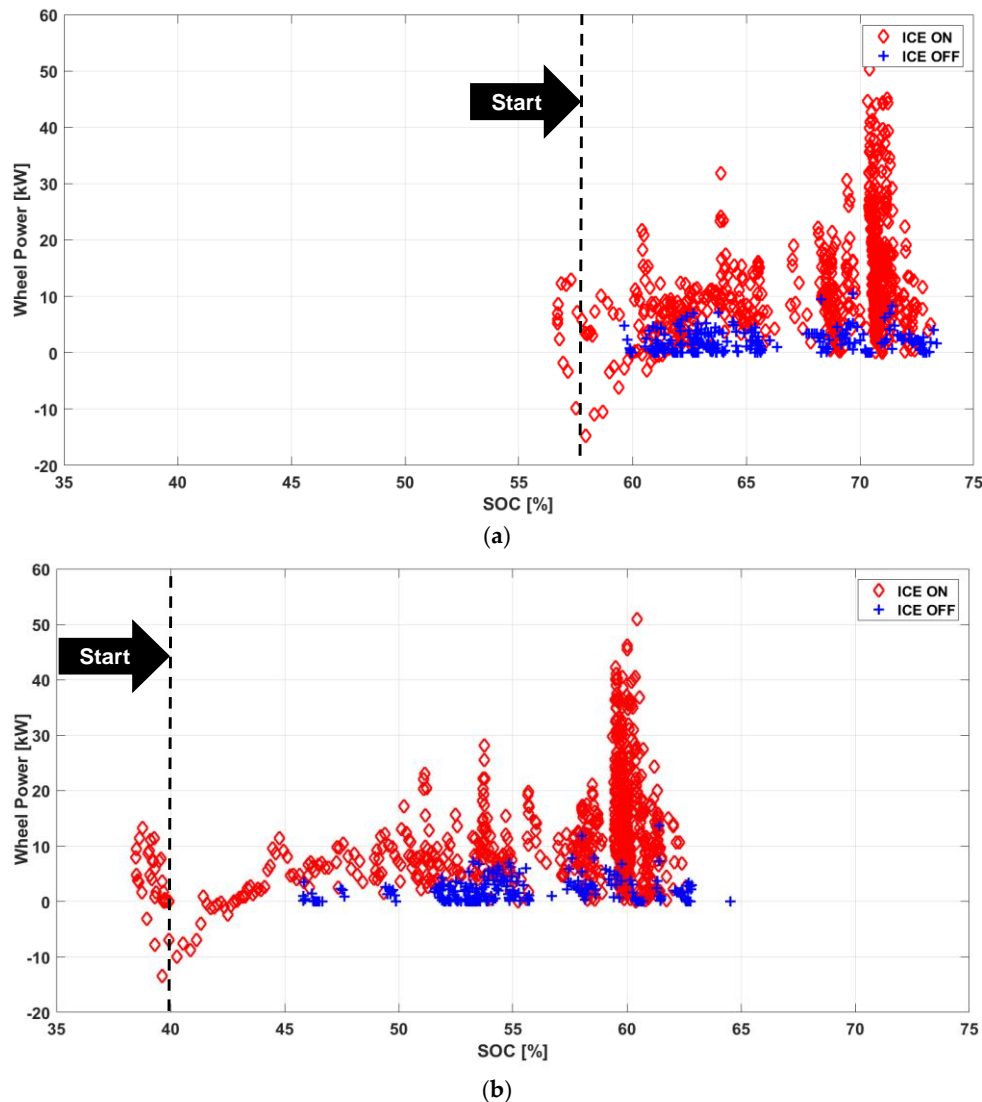


Figure 10. WLTC Cold start: ICE On/Off vs. battery SOC for High SOC (a) and Low SOC (b) cases.

Finally, it can be noticed that in the Low SOC case the EMS limits the electric drive at power levels below 2.5 kW, until SOC values of about 50% are reached.

The same analysis carried out on the NEDC, which is not reported here for sake of brevity, highlighted a similar EMS behavior.

Another important parameter, which plays a key role in the EMS logic, is the product of vehicle speed and acceleration. The analysis of the data recorded on the WLTC, shown in Figure 11, highlights that the electric drive both for the High SOC and Low SOC cases is confined in a well-defined region from -3.5 to $4.5 \text{ m}^2/\text{s}^3$. More specifically, the EMS limits the electric drive to the conditions when:

- Vehicle speeds are in the medium range (below 60 km/h) and the accelerations are very low (below 0.5 m/s^2);
- Accelerations are moderate (below 1 m/s^2) and speeds are low (below 20 km/h) [27].

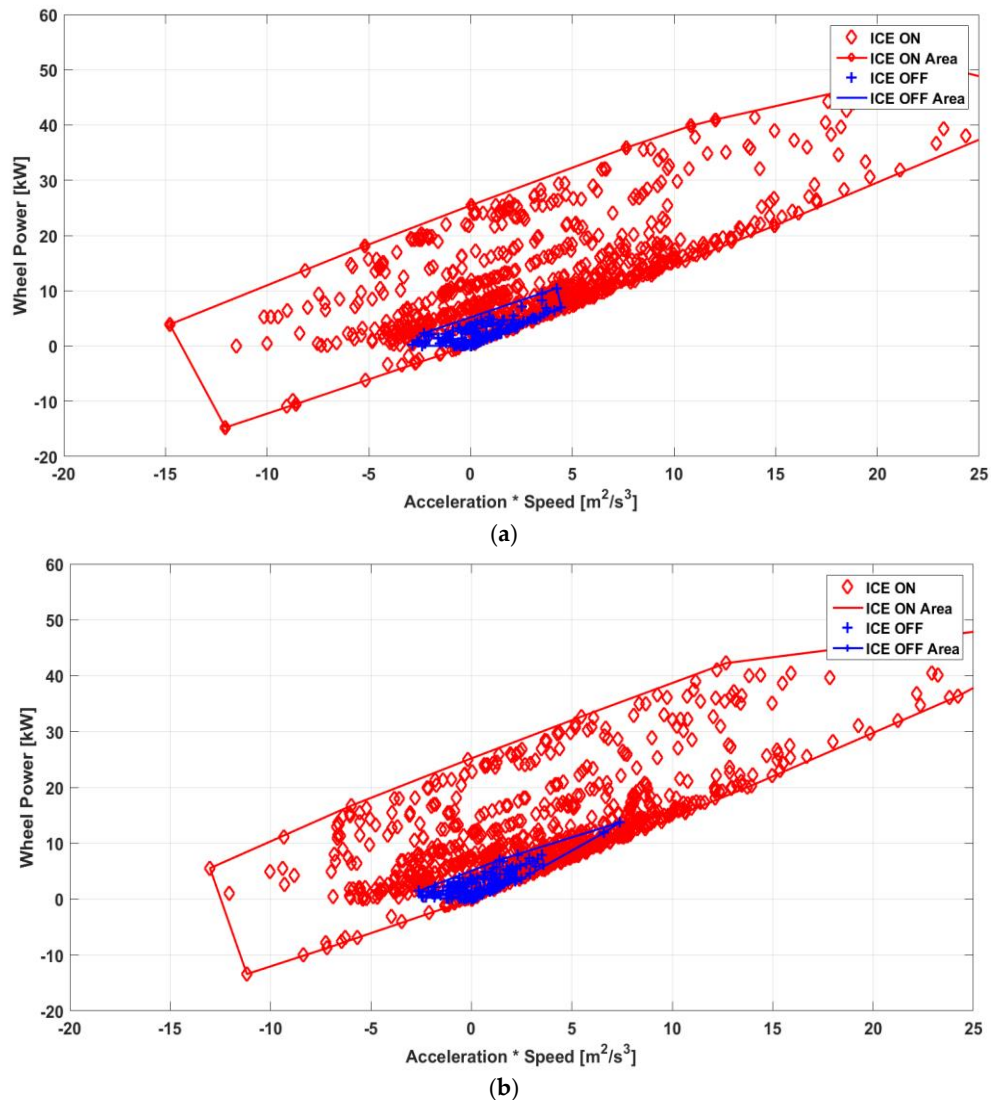


Figure 11. WLTC Cold start: ICE On/Off status vs. the product between vehicle speed and acceleration for High SOC (a) and Low SOC (b) cases.

Finally, further analyses were carried out to characterize in more detail the ICE operation modes during the PH operation. In particular, the SC or the E-Boost can be identified by comparing the battery current signal with the ICE On/Off condition: current flowing from the battery when the ICE is On corresponds to E-Boost, while current flowing into the battery when the ICE is On corresponds to SC. A further operating condition when the engine is On without providing any traction power to the vehicle (such as during vehicle decelerations) can be identified as a “Catalyst Heating” condition, since the main scope of this operation mode is to warm-up the after-treatment system. The same operating points recorded over the WLTC, which were previously shown in Figures 10 and 11, have been plotted in Figures 12 and 13, as a function of SOC and of the product between vehicle speed and acceleration respectively. The square markers represent SC condition, the diamond markers stand for the E-Boost, and the X markers indicate the Cat-Heating.

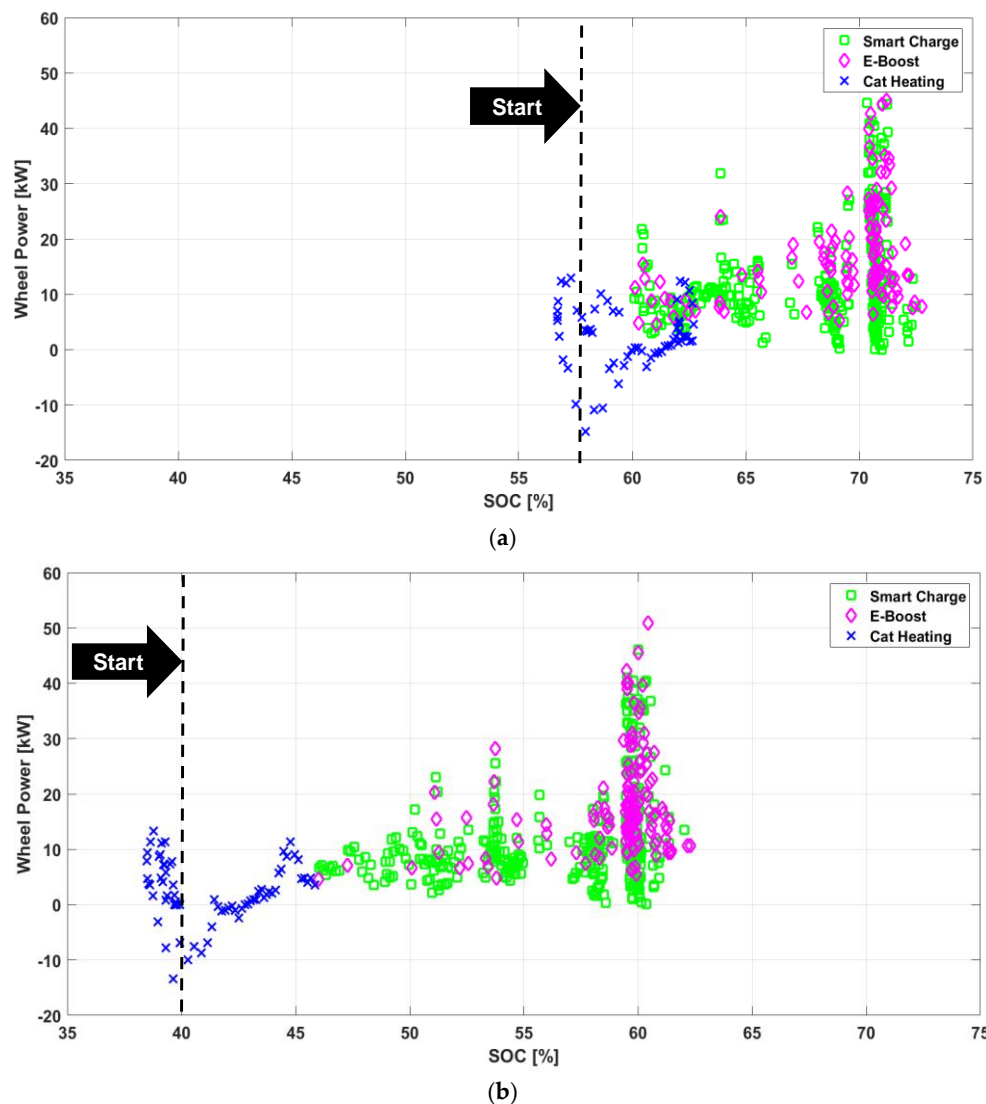


Figure 12. WLTC Cold start: ICE operating conditions for High SOC (a) and Low SOC (b) as a function of battery SOC.

The engine most frequent operating condition is the SC throughout all operating domain, especially when the battery SOC is below 55%, as it is evident from Figure 12, but also the exploitation of the E-Boost for both SOC levels is not negligible for power demands ranging from 10 to 50 kW when the battery SOC is above 60% [27].

The same data, plotted in Figure 13 as a function of the product between vehicle speed and acceleration, confirm the predominance of SC along the WLTC.

Finally, the time share of the different operating modes along the WLTC and the NEDC is reported in Figures 14 and 15, where the term “Other” refers to non-specific operating conditions such as engine cranking, or to the impossibility to associate a measurement to a particular mode due to problems of signal phasing. It is evident that passing from the NEDC to the WLTC the reduction of the electric drive is significant, from 35% to 20%, for the High SOC and from 30% to 17% for the Low SOC.

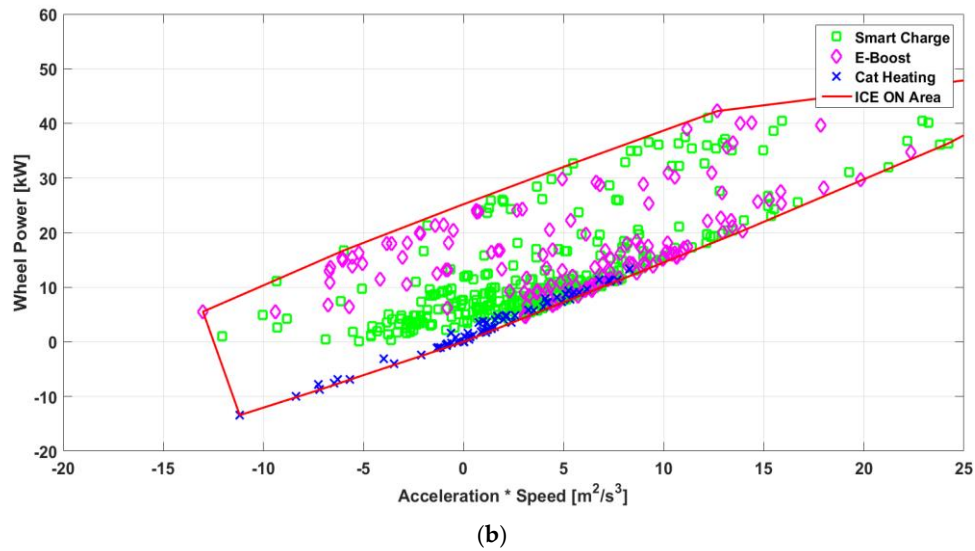
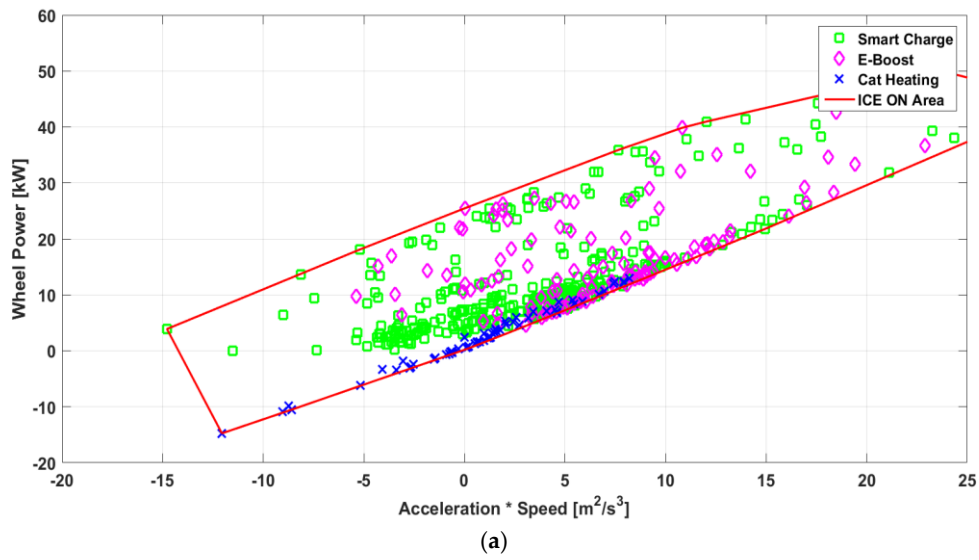


Figure 13. WLTC Cold start—ICE operating conditions for High SOC (a) and Low SOC (b) as a function of the product between vehicle speed and acceleration.

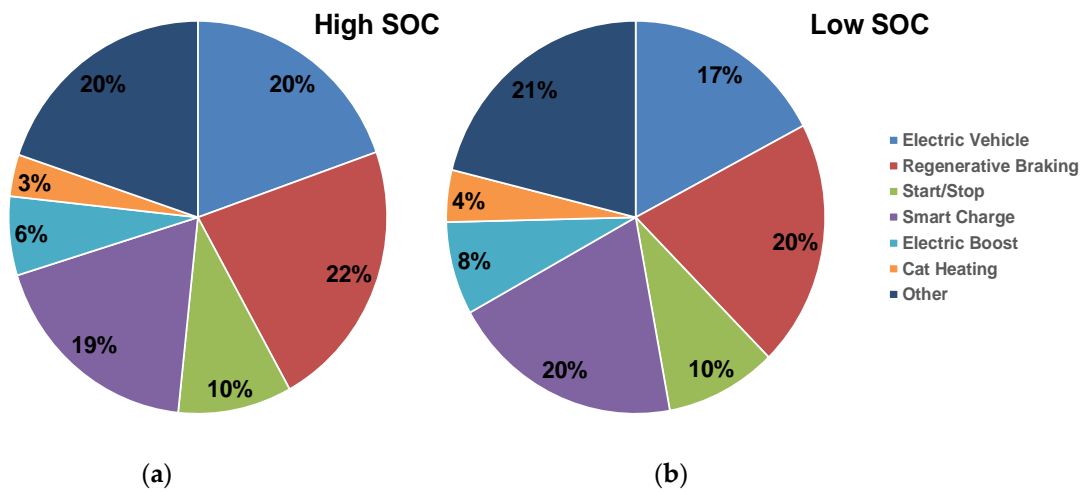


Figure 14. WLTC Cold start—Vehicle operating mode share for High SOC (a) and Low SOC (b) [27].

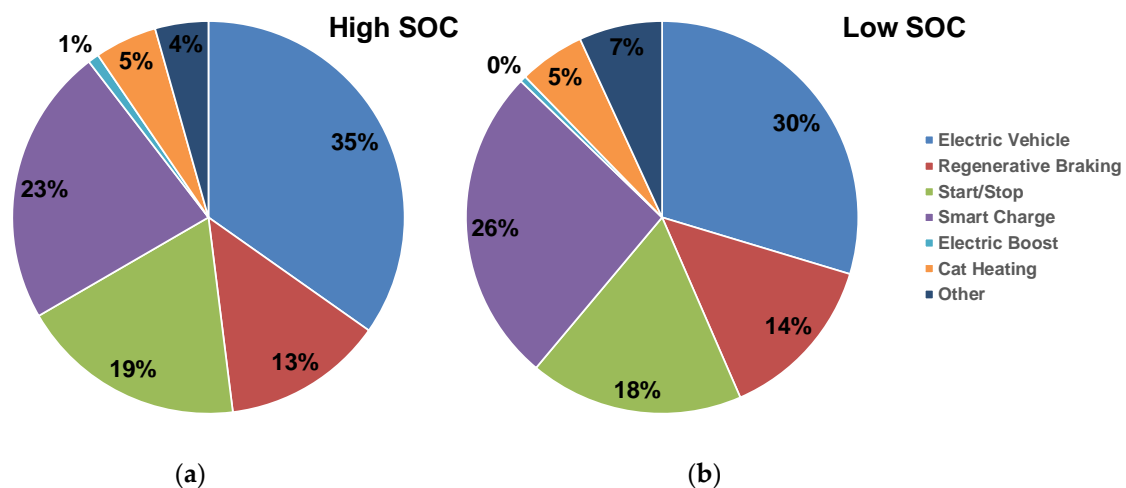


Figure 15. NEDC Cold start - Vehicle operating mode share for High SOC (a) and Low SOC (b) [27].

Moreover, both graphs confirm that the exploitation of the SC mode is wider than the E-Boost, which is almost negligible (below 1%) on the NEDC, since, due to the low power demand of this driving cycle, the EMS constantly tries to increase the load on the ICE to increase its efficiency through the SC. On the WLTC instead, due to the higher power demand of the driving cycle, the exploitation of the E-Boost is not negligible (about 7% of the total time), although still two-three times less frequent than the SC.

Finally, passing from the NEDC to the WLTC will lead to a significant reduction of both the stop-start (from about 19% to 10%) and of the Cat-Heating (from about 5% to about 3%) [27].

3.3. Analysis of the Impact of the Cold Start on the EMS Logics

The effect of Cold start on the EMS logic was then analyzed along the WLTC and NEDC cycles, focusing only on the High SOC case, since similar observations could be done also for the Low SOC test. For a meaningful comparison similar battery SOC values at the beginning of the cycle were considered (between 60 and 70%), as shown in Figure 16. However, it is worth pointing out that, due to the impossibility to recharge externally the battery, it would be almost impossible to guarantee the same initial battery SOC for the different cycles.

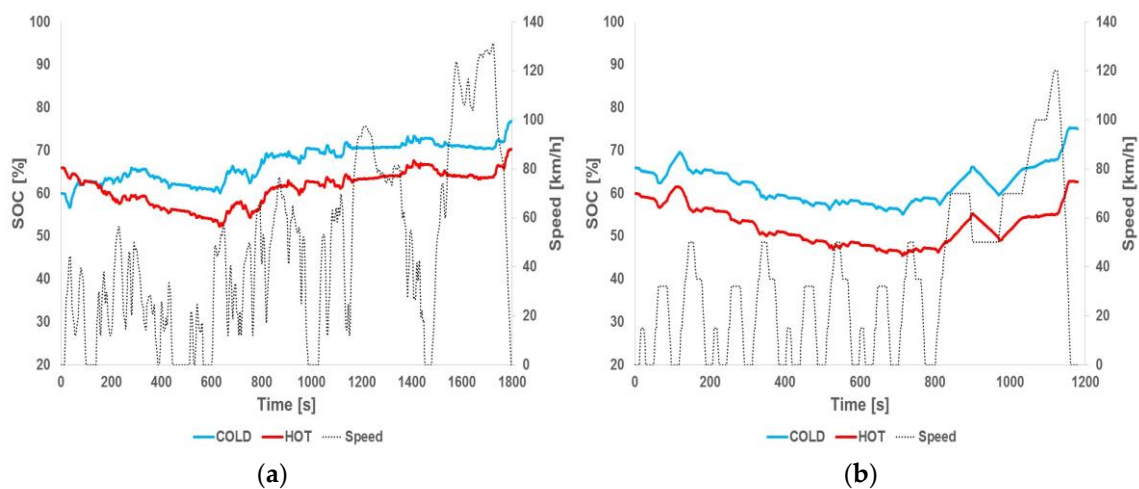


Figure 16. Battery SOC for HOT (Red) and COLD (Blue) start, during WLTC (a) and NEDC (b) for the High SOC case.

As evident from Figure 16, the SOC trends are quite similar for the two different test conditions (i.e., Cold and Hot) over both driving cycles, and the main difference is represented by the engine management at the beginning of the cycles, as highlighted in Figure 17, which compares the engine speed profiles for the two thermal conditions. The fuel cut-off and the engine stop-start are disabled in the first portion of the cycles to fasten the warm-up of the engine and of the after-treatment system. Once the warm-up has been achieved, both for the WLTC and for the NEDC cycles, the engine speed profiles corresponding to Hot and Cold starts are almost perfectly overlapped for both driving cycles.

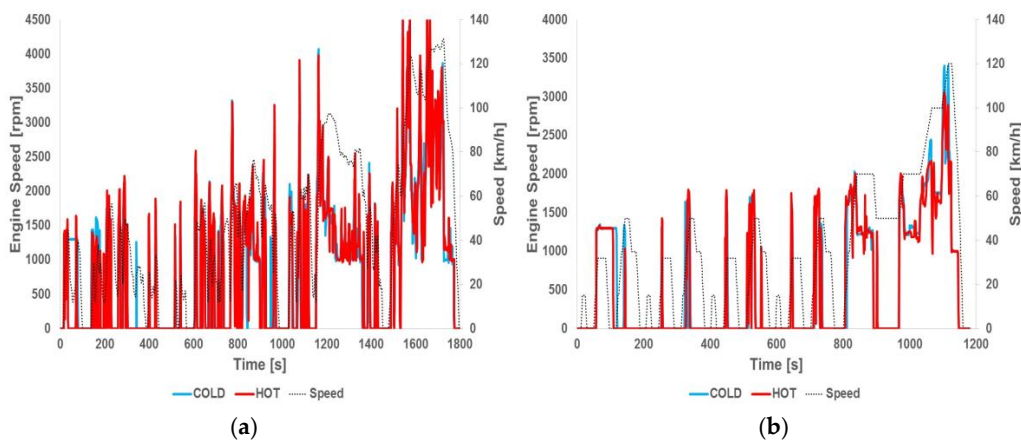


Figure 17. Engine speed for HOT (Red) and COLD (Blue) start, during WLTC (a) and NEDC (b) for the High SOC case.

The pie charts of Figure 18 illustrate the share of the different operating modes along the WLTC and NEDC for the Hot start case. Comparing these results with those reported in Figures 14 and 15 at comparable SOC level, it is possible to observe an extremely limited increase of the electric drive over the WLTC cycle (from 20% to 21% passing from Cold to Hot start conditions), while on the NEDC the effect is more significant (from 35% to 37%). This different behavior can be ascribed to the higher power demand of the WLTP, which requires a more frequent use of the ICE at medium/high loads, leading to a reduction of the warm-up time, to a limited impact of the thermal status of the engine on the electric drive exploitation and on the vehicle CO₂ emissions, as it was already pointed out in Figure 6.

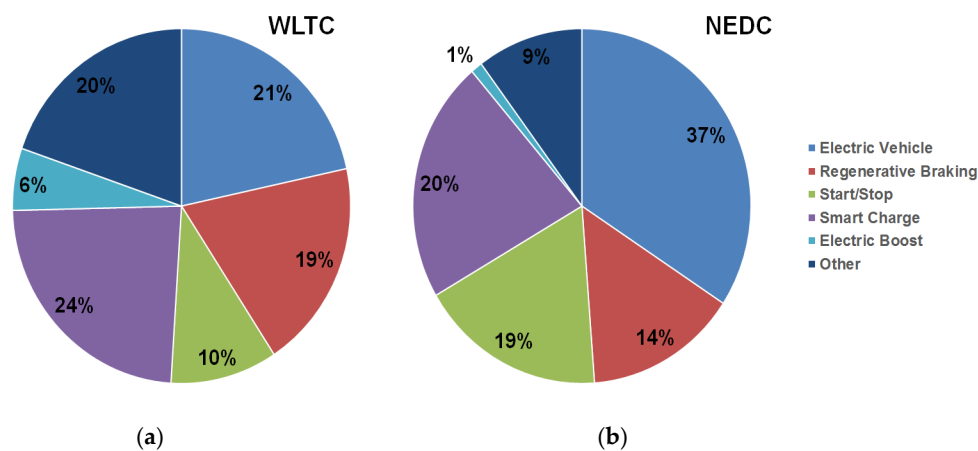


Figure 18. Hot start: vehicle operating mode time-share for WLTC (a) and NEDC (b) cycles for the High SOC case.

4. Conclusions

Experimental tests carried out on a chassis dyno on a Euro 6 HEV, representative of the state of the art hybrid powertrain technology, according to both the current EU TA procedure, based on the NEDC, and the future WLTP procedure, highlighted that, switching from the current NEDC based procedure to the future WLTP procedure:

- The specific energy demand increases of about 50%;
- The electric drive reduces of about 13%, leading to a 30% increase of CO₂ emissions;
- The effect of the Cold start on CO₂ emissions is reduced for WLTP to a percentage growth slightly lower than 4%, from about 12% for the NEDC.

These results demonstrate that the EMS strategies of the tested vehicle can achieve, in test conditions closer to real life such as those corresponding to the WLTP, even higher efficiency levels than those that are currently evaluated on the NEDC, and prove the effectiveness of HEV technology to reduce CO₂ emissions.

Acknowledgments: The valuable support provided to the research activity by the Joint Research Centre is gratefully acknowledged. The authors would like to thank all the staff of the Vehicle Emission LABORATORY (VELA) of the JRC, and in particular Jelica Pavlovic and Ricardo Suarez Bertoa, for their precious and constant contribution to the work.

Author Contributions: Claudio Cubito, Biagio Ciuffo and Simone Serra planned the experimental test campaign for the hybrid vehicle. Marcos Otura Garcia, Germana Trentadue, Claudio Cubito and Simone Serra with the supervision of Biagio Ciuffo carried out the experimental campaign on the hybrid vehicle at the chassis dyno rig. Claudio Cubito, Federico Millo, Giulio Boccardo, Giuseppe Di Pierro and Georgios Fontaras analyzed the experimental data and conducted the analysis on the EMS of the hybrid powertrain.

Conflicts of Interest: The authors declare no conflict of interest.

Acronyms

4WD	Four Wheel Drive
E-Boost	Electric Boost
eCVT	Electric Continuous Variable Transmission
EMS	Energy Management System
EU	European Union
EV	Electric Vehicle
FCV	Fuel Cell Vehicle
HEV	Hybrid Electric Vehicle
ICE	Internal Combustion Engine
JRC	Joint Research Centre
MG	Motor Generator
NEDC	New European Driving Cycle
NiMH	Nickel Metal Hydrate
OBD	On Board Diagnostic
PH	Parallel Hybrid
RL	Road Load
SC	Smart Charge
SI	Spark Ignition
SOC	State Of Charge
TA	Type Approval
VELA	Vehicle Emissions Laboratory
WLTC	Worldwide Harmonized Light duty Test Cycle
WLTP	Worldwide Harmonized Light duty Test Procedure

References

1. European Commission 2050 Low-Carbon Economy. Available online: https://ec.europa.eu/clima/policies/strategies/2050_en (accessed on 7 July 2017).
2. Karamanev, D.; Pupkevich, V.; Penev, K.; Glibin, V.; Gohil, J.; Vajihinejad, V. Biological conversion of hydrogen to electricity for energy storage. *Energy* **2017**, *129*, 237–245. [[CrossRef](#)]
3. Ziogou, C.; Ipsakis, D.; Seferlis, P.; Bezergianni, S.; Papadopoulou, S.; Voutetakis, S. Optimal production of renewable hydrogen based on an efficient energy management strategy. *Energy* **2013**, *55*, 58–67. [[CrossRef](#)]
4. Nastasi, B.; Lo Basso, G. Hydrogen to link heat and electricity in the transition towards future Smart Energy Systems. *Energy* **2016**, *110*, 5–22. [[CrossRef](#)]
5. Perna, A.; Minutillo, M.; Jannelli, E. Hydrogen from intermittent renewable energy sources as gasification medium in integrated waste gasification combined cycle power plants: A performance comparison. *Energy* **2016**, *94*, 457–465. [[CrossRef](#)]
6. Fathabadi, H. Utilization of electric vehicles and renewable energy sources used as distributed generators for improving characteristics of electric power distribution systems. *Energy* **2015**, *90*, 1100–1110. [[CrossRef](#)]
7. Falcão, E.A.M.; Teixeira, A.C.R.; Sodré, J.R. Analysis of CO₂ emissions and techno-economic feasibility of an electric commercial vehicle. *Appl. Energy* **2017**, *193*, 297–307. [[CrossRef](#)]
8. De Gennaro, M.; Paffumi, E.; Martini, G. Customer-driven design of the recharge infrastructure and Vehicle-to-Grid in urban areas: A large-scale application for electric vehicles deployment. *Energy* **2015**, *82*, 294–311. [[CrossRef](#)]
9. Davidov, S.; Pantoš, M. Planning of electric vehicle infrastructure based on charging reliability and quality of service. *Energy* **2016**. [[CrossRef](#)]
10. Vassileva, I.; Campillo, J. Adoption barriers for electric vehicles: Experiences from early adopters in Sweden. *Energy* **2016**, *120*, 632–641. [[CrossRef](#)]
11. Felgenhauer, M.F.; Pellow, M.A.; Benson, S.M.; Hamacher, T. Evaluating co-benefits of battery and fuel cell vehicles in a community in California. *Energy* **2016**, *114*, 360–368. [[CrossRef](#)]
12. Sharma, R.; Manzie, C.; Bessedé, M.; Crawford, R.H.; Brear, M.J. Conventional, hybrid and electric vehicles for Australian driving conditions. Part 2: Life cycle CO₂-e emissions. *Transp. Res. Part C Emerg. Technol.* **2013**, *28*, 63–73. [[CrossRef](#)]
13. Mishina, Y.; Muromachi, Y. Are potential reductions in CO₂ emissions via hybrid electric vehicles actualized in real traffic? The case of Japan. *Transp. Res. Part D Transp. Environ.* **2017**, *50*, 372–384. [[CrossRef](#)]
14. Millo, F.; Rolando, L.; Servetto, E. Development of a control strategy for complex light-duty diesel-hybrid powertrains. In Proceedings of the 10th International Conference on Engines & Vehicles, Capri, Italy, 11–15 September 2011. [[CrossRef](#)]
15. Millo, F.; Badami, M.; Ferraro, C.V.; Rolando, L. Different Hybrid Powertrain Solutions for European Diesel passenger cars. *SAE Int. J. Engines* **2010**, *2*, 493–504. [[CrossRef](#)]
16. Millo, F.; Badami, M.; Ferraro, C.V.; Lavarino, G.; Rolando, L. A comparison between different hybrid powertrain solutions for an European mid-size passenger car. *SAE Tech. Pap.* **2010**. [[CrossRef](#)]
17. UNECE Regulation No. 83: Uniform Provisions Concerning the Approval of Vehicles with Regard to the Emission of Pollutants According to Engine Fuel Requirements. Available online: [http://eur-lex.europa.eu/legal-content/EN/TXT/?uri=CELEX:42012X0215\(01\)](http://eur-lex.europa.eu/legal-content/EN/TXT/?uri=CELEX:42012X0215(01)) (accessed on 3 May 2017).
18. UNECE Regulation No. 101 Uniform Provisions Concerning the Approval of Passenger Cars Powered by an Internal Combustion Engine Only, or Powered by a Hybrid Electric Power Train with Regard to the Measurement of the Emission of Carbon Dioxide and Fuel Consumption. Available online: <http://www.unece.org/trans/main/wp29/wp29wgs/wp29gen/wp29fdocstts.html> (accessed on 3 May 2017).
19. Mock, P.; German, J.; Bandivadekar, A.; Riemersma, I. Discrepancies between Type-Approval and “Real-World” Fuel-Consumption and CO₂ Values. Available online: http://www.theicct.org/sites/default/files/publications/ICCT_EU_fuelconsumption2_workingpaper_2012pdf (accessed on 4 May 2017).
20. Mock, P.; Tietge, U.; Franco, V.; German, J.; Bandivadekar, A.; Ligterink, N.; Lambrecht, U.; Kühlwein, J.; Riemersma, I. From Laboratory to Road—A 2014 Update of Official and “Real-World” Fuel Consumption and CO₂ Values for Passenger Cars in Europe. Available online: http://www.theicct.org/sites/default/files/publications/ICCT_LaboratoryToRoad_2014_Report_English.pdf (accessed on 24 January 2017).

21. United Nations. *Addendum 15: Global Technical Regulation No. 15—Worldwide Harmonized Light Vehicles Test Procedure*; UNECE: Geneva, Switzerland, 2015; Volume ECE/TRANS/, pp. 1–234.
22. Cubito, C.; Rolando, L.; Millo, F.; Ciuffo, B.; Serra, S.; Trentadue, G.; Marcos Garcia, O.; Fontaras, G. Energy Management Analysis under Different Operating Modes for a Euro-6 Plug-in Hybrid Passenger Car. *SAE Tech. Pap.* **2017**. [[CrossRef](#)]
23. Badin, F.; Le Berr, F.; Castel, G.; Dabadie, J.C.; Briki, H.; Degeilh, P.; Pasquier, M. Energy efficiency evaluation of a Plug-in Hybrid Vehicle under European procedure, Worldwide harmonized procedure and actual use. In Proceedings of the EVS28 International Electric Vehicle Symposium and Exhibition, KINTEX, Goyang, Korea, 3–6 May 2015; pp. 1–14.
24. Kim, N.; Rask, E.; Rousseau, A. Control Analysis under Different Driving Conditions for Peugeot 3008 Hybrid 4. *SAE Tech. Pap.* **2014**. [[CrossRef](#)]
25. Kim, N.; Duoba, M.; Kim, N.; Rousseau, A. Validating Volt PHEV Model with Dynamometer Test Data Using Autonomie. *SAE Int.* **2013**, *6*, 985–992. [[CrossRef](#)]
26. Rousseau, J.; Kwon, P.; Sharer, S.; Pagerit, M. Duoba Integrating Data, Performing Quality Assurance, and Validating the Vehicle Model for the 2004 Prius Using PSAT. In Proceedings of the 2006 SAE World Congress & Exhibition, Detroit, MI, USA, 3–6 April 2006. [[CrossRef](#)]
27. Cubito, C. A Policy-Oriented Vehicle Simulation Approach for Estimating the CO₂ Emissions from Hybrid Light Duty Vehicles. Ph.D. Thesis, Politecnico di Torino, Torino, Italy, 2017.
28. Lukic, S.M.; Member, S.; Cao, J.; Bansal, R.C.; Member, S.; Rodriguez, F.; Emadi, A. Energy Storage Systems for Automotive Applications. *IEEE Trans. Ind. Electron.* **2008**, *55*, 2258–2267. [[CrossRef](#)]
29. Krein, P.T. Battery Management for Maximum Performance in Plug-In Electric and Hybrid Vehicles. In Proceedings of the Vehicle Power and Propulsion Conference, Arlington, TX, USA, 9–12 September 2007; pp. 2–5.
30. Taniguchi, A.; Fujioka, N.; Ikoma, M.; Ohta, A. Development of nickel/metal-hydride batteries for EVs and HEVs. *J. Power Sources* **2001**, *100*, 117–124. [[CrossRef](#)]
31. Pavlovic, J.; Marotta, A.; Ciuffo, B.; Serra, S.; Fontaras, G.; Anagnostopoulos, K.; Tsiakmakis, S.; Arcidiacono, V.; Hausberger, S.; Silberholz, G. Correction of Test Cycle Tolerances: Evaluating the Impact on CO₂ Results. *Transp. Res. Procedia* **2016**, *14*, 3099–3108. [[CrossRef](#)]
32. Pavlovic, J.; Marotta, A.; Ciuffo, B. CO₂ emissions and energy demands of vehicles tested under the NEDC and the new WLTP type approval test procedures. *Appl. Energy* **2016**, *177*, 661–670. [[CrossRef](#)]
33. Mock, P.; Kühlwein, J.; Tietge, U.; Franco, V.; Bandivadekar, A.; German, J. The WLTP: How a New Test Procedure for Cars Will Affect Fuel Consumption Values in the EU. Available online: http://www.theicct.org/sites/default/files/publications/ICCT_WLTP_EffectEU_20141029.pdf (accessed on 12 December 2016).



© 2017 by the authors. Licensee MDPI, Basel, Switzerland. This article is an open access article distributed under the terms and conditions of the Creative Commons Attribution (CC BY) license (<http://creativecommons.org/licenses/by/4.0/>).